Journal of Applied Mechanics and Technical Physics, Vol. 43, No. 6, pp. 823–829, 2002

NONBOUSSINESQ THERMAL CONVECTION IN MICROGRAVITY UNDER NONUNIFORM HEATING

Yu. A. Gaponenko[1] **and V. E. Zakhvataev**[2]

UDC 532.529.2:536.412:532.5.013.13

The model of subsonic flows is used to numerically the effect of thermal expansion of a fluid on the formation of naturally convective flows for small Rayleigh numbers (microconvection) and spatially periodic distribution of heat flows on the boundaries of the domain occupied by the fluid.

Introduction. Under low gravity, the formation of free convection can be strongly affected by small changes in the thermal properties of the medium, which are insignificant under ground conditions. In particular, theoretically, volume expansion can cause some convective phenomena observed in experiments performed aboard spacecraft [1, 2].

Estimates of the orders of magnitudes in the complete Navier–Stokes and heat-transfer equations and numerical studies show that if the Rayleigh number R is small enough [3, 4], i.e.,

$$\mathrm{R}/\varepsilon \equiv gH^3/(\nu\chi) \leqslant O(1), \tag{1}$$

the contribution of the density changes due to thermal expansion of the medium to the formation of the velocity field is comparable to or exceeds the contribution of buoyancy forces. In this case, the Oberbeck–Boussinesq approximation is inapplicable for description of thermal convection. In (1), $\varepsilon = \beta\Delta T$ is the Boussinesq parameter (ΔT is the typical temperature difference and β is the temperature coefficient of volume expansion), H is the characteristic linear dimension, g is the acceleration of the external force field, ν is the kinematic viscosity, and χ is the thermal diffusivity of the medium at a certain characteristic temperature. Conditions (1) hold under microacceleration achievable aboard modern spacecraft. The convective flows formed under conditions (1) and usually characterized by velocities of about 10 μm/sec and lower are called microconvection [4].

Microconvection can be described using the well-known model of substantially subsonic flows with arbitrary density changes, which is obtained from the complete system of Navier–Stokes and heat-transfer equations in the limit as the Mach number and hydrostatic compressibility tend to zero [5, 6].

In previous studies of microconvection [3, 4, 7–12], the basic model was the model of microconvection, which is essentially a particular case of the subsonic flow approximation. Emphasis was given to investigating the effect of external actions changing rapidly in time because they can cause a marked changes in the density of the medium. The creation of rapidly changing heating conditions underlay some experiments on detection and investigation of microconvection phenomena.

For experimental investigation of microconvection, it is proposed to use spatially nonuniform heating, which allows the structure and characteristics of convective flows to be easily controlled by means of thermal expansion of the medium. In the present study, we consider the effect of spatially periodic heating on the formation of microconvection in a rectangle. The dependence of the structure and properties of microconvective flows of this type on the physical and geometrical constitutive parameters is studied numerically.

[1]Institute of Computational Simulation, Siberian Division, Russian Academy of Sciences, Krasnoyarsk 660036. [2]Siberian State Technological University, Krasnoyarsk 660049. Translated from Prikladnaya Mekhanika i Tekhnicheskaya Fizika, Vol. 43, No. 6, pp. 46–53, November–December, 2002. Original article submitted June 18, 2001; revision submitted February 4, 2002.

0021-8944/02/4306-0823 $27.00

Formulation of the Problem. We consider two-dimensional microconvective fluid flows with isobaric volume-expansion coefficient β, viscosity μ, thermal conductivity k, and specific heat at constant pressure c_P (volumetric viscosity is set equal to zero); it is assumed that the above-mentioned thermal properties are constant. The fluid occupies a rectangular domain $0 \leqslant x \leqslant L$, $0 \leqslant y \leqslant H$ bounded by solid impermeable walls (x and y are Cartesian axes). The system is in a constant homogeneous external force field, and the direction of the vector $\boldsymbol{g}$ of acceleration of the external mass forces coincides with the x axis. The state of the system is described by following fields: the field of density $\rho(\boldsymbol{x}, t)$ at the time t at the point $\boldsymbol{x} = (x, y)$, the velocity field $\boldsymbol{v}(\boldsymbol{x}, t) = (v_1, v_2)$, the pressure $p(\boldsymbol{x}, t)$, and the deviation of the temperature θ from the characteristic value θ_0 — $T(\boldsymbol{x}, t) = \theta - \theta_0$.

Initially, all walls, except for $y = 0$, are heat insulated. Beginning at a certain time, a heat flow which changes periodically in time and space is specified on the boundary of the domain $y = 0$:

$$T_y = \Theta \cos(\omega t) \cos(nx\pi/L). \tag{2}$$

Here ω is the frequency of fluctuations of the heat flow and n is the number of fluctuation half-periods of the heat flow. The heat-insulation conditions or condition (2) is specified on the boundary $y = H$. The walls $x = 0$ and $x = L$ remain heat insulated.

The flows considered are described using the model of subsonic flows. We note that in the subsonic flow approximation, the total pressure is written as the sum of the spatially homogeneous thermodynamic component $P(t)$ and the component $p(\boldsymbol{x}, t)$ that takes into account the dynamic and hydrostatic effects; the latter is eliminated from the equation of state, which ensures "filtration" of the acoustics. In the case considered, by virtue of the boundary conditions (the total conductive heat flow through the boundary of the domain is equal to zero) $P = \text{const}$, and the equations of the subsonic flow model become

$$-\frac{1}{\rho}\frac{d\rho}{dt} = \nabla \cdot \boldsymbol{v}, \qquad \rho \frac{d\boldsymbol{v}}{dt} = -\nabla p + \frac{\mu}{3}\nabla(\nabla \cdot \boldsymbol{v}) + \mu \nabla^2 \boldsymbol{v} + \rho \boldsymbol{g}, \qquad \rho c_P \frac{dT}{dt} = k\nabla^2 T. \tag{3}$$

As the equation of state, we use the linear dependence of the specific volume on temperature [3, 4]

$$\rho = \rho_0 (1 + \beta T)^{-1}, \tag{4}$$

where $\rho_0 > 0$ is the characteristic (constant) density.

Combining the continuity and heat equations and the equation of state, we obtain

$$\nabla \cdot \boldsymbol{v} = \beta \chi \nabla^2 T, \tag{5}$$

where $\chi = k/(\rho_0 c_P)$ is the thermal diffusivity.

System (3)–(5) corresponds to the microconvection model [3, 4] in the physical variable obtained from the equations of linear nonequilibrium thermodynamics by *a priori* assumptions in [3].

The scales for the distance, velocities, time, modified pressure, and temperature are H, $\varepsilon\chi/H$, H^2/χ, $\rho_0(\varepsilon\nu\chi/H)^2$, and $\Theta H = \Delta T$, respectively. Then, in the dimensionless variables, system (3)–(5) take the following form: ($0 \leqslant x \leqslant A$ and $0 \leqslant y \leqslant 1$):

$$\nabla \cdot \boldsymbol{v} = \varepsilon \nabla^2 T,$$

$$\mathrm{Pr}^{-1}\Big(\frac{\partial \boldsymbol{v}}{\partial t} + \varepsilon \boldsymbol{v} \cdot \nabla \boldsymbol{v}\Big) = \mathrm{G} T \boldsymbol{k} - (1 + \varepsilon T)\nabla p + (1 + \varepsilon T)\nabla \cdot \boldsymbol{T}, \tag{6}$$

$$\frac{\partial T}{\partial t} + \varepsilon \boldsymbol{v} \cdot \nabla T = (1 + \varepsilon T)\nabla^2 T.$$

Here $\mathrm{G} = |\boldsymbol{g}|H^3/(\nu\chi)$ is the Galilei number, $\mathrm{Pr} = \nu/\chi$ is the Prandtl number, $A = L/H$ is the aspect ratio, $\boldsymbol{T}$ is the Cartesian tensor with the components $T_{ik} = \partial v_i/\partial x_k + \partial v_k/\partial x_i - (2/3)\delta_{ik}\nabla \cdot \boldsymbol{v}$, and $\boldsymbol{k} = \boldsymbol{g}/|\boldsymbol{g}|$.

Two versions of boundary conditions for temperature are used. The boundary conditions are as follows: for one-sided heating,

$$x = 0,\ x = A\text{:} \quad T_x = 0; \tag{7}$$

$$y = 1\text{:} \quad T_y = 0, \qquad y = 0\text{:} \quad T_y = \cos(\omega t)\cos(\pi n x/A); \tag{8}$$

and for two-sided heating, relation (7) and

$$y = 0,\ 1\text{:} \quad T_y = \cos(\omega t)\cos(\pi n x/A). \tag{9}$$

TABLE 1

Fluid No.	χ, cm^2/sec	β, K^{-1}	Pr
1	0.001518	0.0002	5.4
2	0.001098	0.0010	838.0
3	0.001120	0.0010	1625.0
4	0.490000	$7.5 \cdot 10^{-6}$	0.0054

For the velocity on the boundary of the calculation domain, the attachment conditions are specified:

$$\boldsymbol{v} = 0. \tag{10}$$

The initial data correspond to the equilibrium state:

$$t = 0: \quad \boldsymbol{v} = 0, \quad T = T_0. \tag{11}$$

The temperature field is determined by solving the heat-conductivity equation $T_{0t} = \nabla^2 T_0$ subject to boundary conditions (7)–(11).

The results of numerical solution of problem (6)–(11) are compared with the results of solution of a similar problem in the Oberbeck–Boussinesq approximation. The corresponding equation and the boundary conditions for the Oberbeck–Boussinesq model can be obtained by setting $\varepsilon = 0$ in the continuity equation in system (6)and in the factor $1 + \varepsilon T$.

Equations (6) are solved by a finite-difference method designed using the well-known method [13] and one of its modifications for compressible flows [5]. For transition from the nth to the $(n+1)$th time layer, the following procedure is used.

1. The approximate value of the velocity $\boldsymbol{v}_1^{n+1}$ is determined by scalar marching along each of the x and y directions:

$$\boldsymbol{v}_1^{n+1} = \boldsymbol{v}^n + \tau[-\varepsilon \boldsymbol{v}^n \cdot \nabla \boldsymbol{v}_1^{n+1} - (1 + \varepsilon T^n)\mathrm{Pr}\nabla p^n + (1 + \varepsilon T^n)\nabla \cdot \boldsymbol{T}_1^{n+1} + \mathrm{G}T^n g\boldsymbol{k}].$$

2. The pressure p and refined velocity $\boldsymbol{v}$ are calculated by an iterative procedure (k is the iteration number):

$$p_k^{n+1} = p_{k-1}^{n+1} - \gamma(\nabla \boldsymbol{v}_k^{n+1} - \varepsilon \nabla^2 T^n),$$

$$\boldsymbol{v}_{k+1}^{n+1} = \boldsymbol{v}_k^{n+1} - \tau(1 + \varepsilon T^n)\mathrm{Pr}(\nabla p_k^{n+1} - \nabla p_{k-1}^{n+1}).$$

The iterations continue until the inequality $|p_k^{n+1} - p_{k-1}^{n+1}| < \varepsilon_p$ (ε_p is the specified calculation accuracy) is satisfied. The initial pressure for the iterations is $p_0^{n+1} = p^n$. The parameter γ, characterizing the rate of convergence of the process, is set equal to

$$\gamma = \frac{1}{\tau \mathrm{Pr}(1 + \varepsilon T^n)} \Big(\frac{2}{h_x^2} + \frac{2}{h_y^2} \Big)^{-1}.$$

3. The temperature T^{n+1} is determined from the energy equation by scalar marching:

$$T^{n+1} = T^n - \tau \varepsilon \boldsymbol{v}^{n+1} \cdot \nabla T^{n+1} + \tau(1 + \varepsilon T^n)\nabla^2 T^{n+1}.$$

This computational algorithm is implemented using a grid composed of a main system of nodes (for p and T) and two auxiliary systems of nodes (for each of the velocity components) [5, 13]. The spatial derivatives are approximated by central differences with second-order accuracy. The derivatives on the domain boundary are calculated using "fictitious" cells outside the computational grid, in which the required quantities are calculated by means of quadratic extrapolation.

The calculation accuracy was checked by the maximum balance of mass in a cell for the entire computation domain

$$E_m = \int \rho|_{\rho(t)}\, dx\, dy - \int \rho|_{\rho(0)}\, dx\, dy + \int \rho \boldsymbol{v}\, dS\, dt,$$

which was maintained within $\pm 1\%$.

Results of Numerical Modeling and Discussion. The present calculations of convective flows are performed for fluids whose parameters are given in Table 1. We consider model media such as water H_2O (fluid No. 1), PMS-100 (fluid No. 2) and PMS-200 (fluid No. 3) silicone oils at a temperature of 300 K [14], and a medium

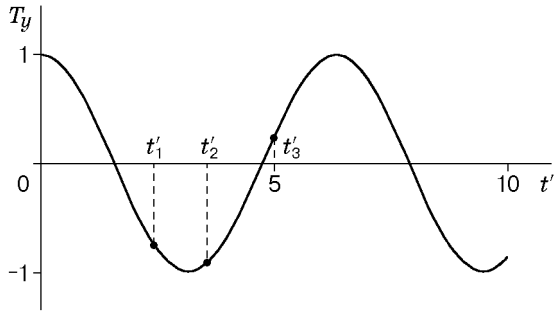

Fig. 1. Temperature versus time.

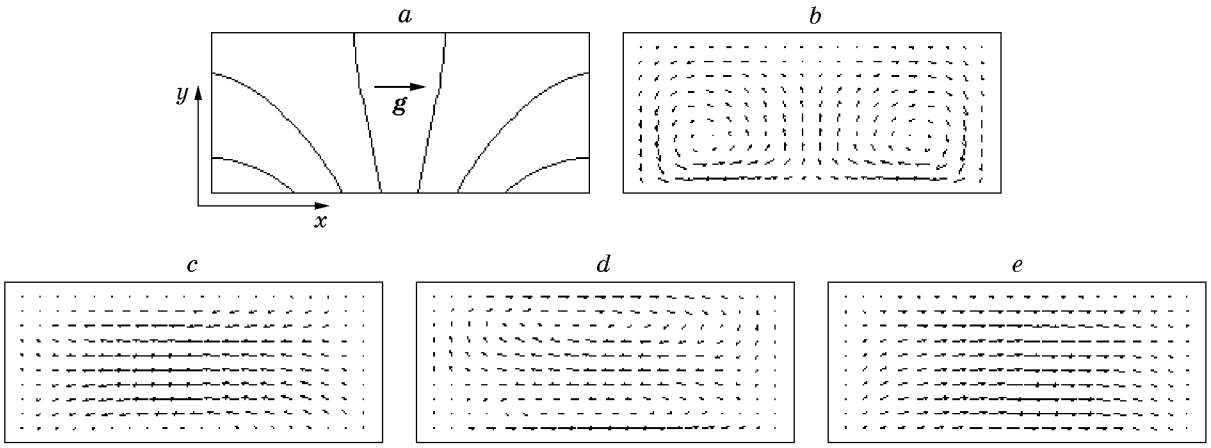

Fig. 2. Temperature isolines (a) and velocity fields for the Oberbeck–Boussinesq model (b) and the microconvection model for $t' = t'_1$ (c), $t' = t'_2$ (d), and $t' = t'_3$ (e).

with a small Prandtl number, such as a molten metal or a semiconductor (No. 4). The space scale is $H = 1$ cm, and the dimensionless angular frequency of fluctuations of the heat flow through the boundary $\omega' = 1$.

We study the mechanisms of formation of microconvective flows, the dependence of their structure and properties on the constitutive parameters under nonstationary, spatially periodic distribution of heat flow on the boundaries of the closed domain occupied by the fluid. A main parameter of the problem that determines the extent to which the velocity field is affected by the buoyancy force and volume expansion is the Galilei number $\mathrm{G} = \mathrm{R}/\varepsilon$ (microconvection parameter [3, 4]).

Case of Absence of External Forces. The effect of thermal expansion of the fluid is most pronounced in the absence of external force fields. In this case, the single external factor that can induce macroscopic motion is the nonstationary nonuniform thermal action on the walls of the cavity, and the occurrence of convection is only related to the thermal expansion of the fluid. The mechanism of development of microconvective flow is as follows. Thermal expansion, taken into account by the right side of Eq. (5) $\beta\chi\nabla^2 T$, induces flow as a necessary condition for conservation of mas. In turn, the difference of the quantity $\nabla^2 T$ from zero is due to the nonstationary temperature variations in time and the temperature and velocity field configurations for which $\boldsymbol{v} \cdot \nabla T$ is substantially different from zero in some parts of the domain occupied by the fluid.

Influence of the Microconvection Parameter G *on Microconvective Flow.* In experiments aboard modern spacecraft, the parameter G is substantially different from zero. Numerical calculations confirm that for rather small G, according to (1), thermal expansion dominates. The calculations were performed for the following flow parameters of fluid No. 4: $\mathrm{G} = 0.01$, $A = 2$, $n = 1$, and $\varepsilon = 7.5 \cdot 10^{-4}$. Figure 1 shows a curve of the temperature $T_y\Big|_{x=0}$ versus time. Typical flow structures calculated for the Oberbeck–Boussinesq microconvection model are presented in Fig. 2. Figure 2 shows the temperature isolines at the initial time, the velocity field with a two-vortex symmetric structure typical of the Oberbeck–Boussinesq model, and the velocity field for the microconvection model for various times. According to the results for the microconvection model given here, there are regimes

TABLE 2

Model	$V_{\max}$, cm/sec	
	G = 0.01	G = 1
Microconvection	$1.09 \cdot 10^{-4}$	$1.10 \cdot 10^{-4}$
Oberbeck–Boussinesq	$3.55 \cdot 10^{-9}$	$3.57 \cdot 10^{-7}$

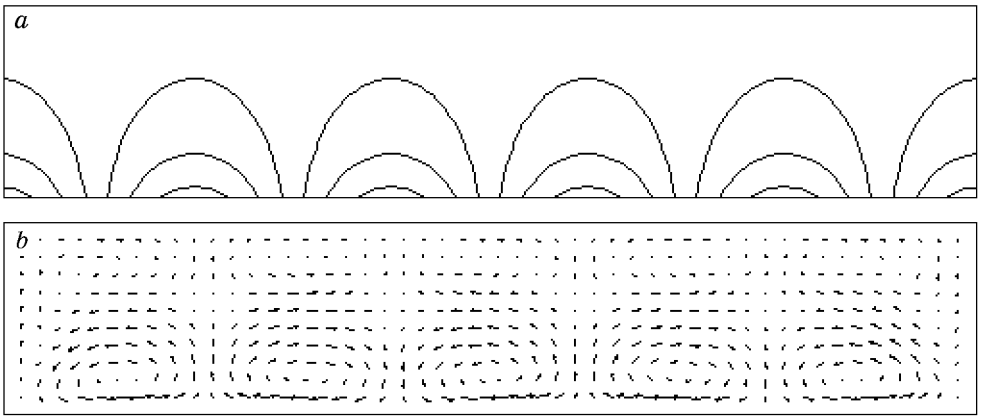

Fig. 3. Temperature isolines (a) and velocity field (b).

of unidirectional flow from the heated to the cooled domain induced by volume expansion (Fig. 2c and e). The formation of such flows occurs at the moments when the temperature field varies in time most dynamically; only when the time-dependent heat flow through the boundary is close to the extreme value, does a two-vortex flow structure (Fig. 2d) form, for which the compressed fluid (by virtue of the continuity equation) flows out from the domain of greater density (compare Fig. 2c–e).

The qualitative difference between the flow structures calculated by the microconvection and Oberbeck–Boussinesq models is obvious: for the latter, the formation of a symmetric two-vortex structure (Fig. 2b) occurs only under the action of the buoyancy force. In this case, as the temperature field varies with time, the centers of the vortices are practically immobile but the direction of rotation changes. In addition, the maximum velocities calculated for theses models differ considerably, especially for small values of G. The maximum velocities for fluid No. 4 at $A = 2$, $n = 1$, and $\Theta = 100$ K/cm are given in Table 2.

Effect of the Spatial Structure of the External Heat Flow on Microconvective Flow. The spatial inhomogeneity of the external temperature field has a decisive effect on the microconvective flow structure. Let us consider the effect of the number of fluctuation half-periods of the temperature gradient on the wall n on microconvection characteristics. Figure 3 shows calculation results for flow of fluid No. 4 with number of fluctuation half-periods T_y on the wall $n = 5$ at G = 0.01, $A = 5$, $\varepsilon = 7.5 \cdot 10^{-4}$. Usually, for rather large A, one fluctuation half-period T_y generates one two-vortex cell in the fluid. Therefore, Fig. 3 shows five two-vortex structures, each of which is induced by one half-period of heat flow fluctuations on the boundary. The calculations show that as n increases, the flow rate decreases; for example, for fluid No. 4, $V_{\max} = 6.05 \cdot 10^{-4}$, $1.8 \cdot 10^{-4}$, and $1.9 \cdot 10^{-5}$ cm/sec at $n = 1$, 2, and 5, respectively. (We note that the maximum temperature gradient in the domain decrease with increase in n.)

Two-Sided Heating. The effect of two-sided heating on the flow structure is shown in Fig. 4, which gives calculation results for fluid No. 4 [subject to boundary conditions (7) and (9)] for $n = 1$, G = 0.01, $A = 2$, and $\varepsilon = 7.5 \cdot 10^{-4}$. The variation in the temperature profile considerably changes the flow structure for the microconvection model. As is evident from Fig. 4, a four-vortex structure is formed in the cavity. The most intense vortices are observed at the heat-insulated walls, i.e., where the temperature field has the highest gradient. However, this leads to a decrease in the maximum velocity: $V_{\max} = 3.02 \cdot 10^{-5}$ cm/sec, whereas for the one-vortex structure, $V_{\max} = 1.09 \cdot 10^{-4}$ cm/sec. This is related to the smaller temperature gradient than that under one-sided heating.

Effect of the Aspect Ratio A on Microconvective Flow. Numerical calculations show that an increase in the aspect ratio leads to an increase in maximum velocity; for example, for fluid No. 4, $V_{\max} = 1.89 \cdot 10^{-5}$, $1.09 \cdot 10^{-4}$, and $6.04 \cdot 10^{-4}$ cm/sec for $A = 1$, 2, and 5 respectively. This effect is related to an increase in the specific power of heating and the temperature gradient increasing with increase in A. In addition, as A increases, the formation

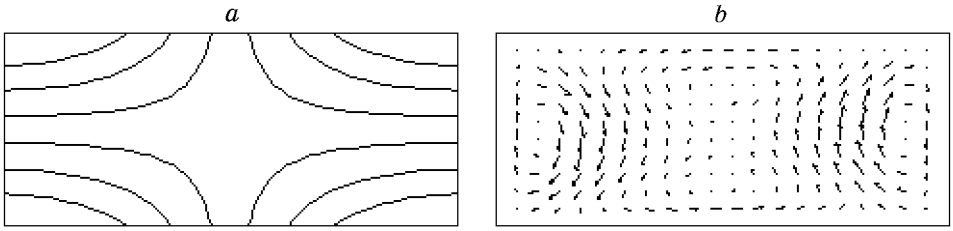

Fig. 4. Temperature isolines (a) and velocity field (b) under two-sided heating.

TABLE 3

Fluid No.	$V_{\max}$, cm/sec	
	$A = 1$	$A = 2$
1	$7.82 \cdot 10^{-7}$	$5.23 \cdot 10^{-6}$
2	$2.31 \cdot 10^{-6}$	$1.65 \cdot 10^{-5}$
3	$2.53 \cdot 10^{-6}$	$1.83 \cdot 10^{-5}$

of the two-vortex structure for the microconvection model occurs at different times: the larger A, the later this formation, compared to the moment when the heat flow on the boundary reaches the extreme value. This may be due to the inertia of the fluid, which counteracts the thermal expansion with reversal of the direction of the boundary heat flow.

The calculation results for fluids Nos. 1, 2, and 3 differ only quantitatively. The maximum velocities $V_{\max}$ for the given fluids at $\mathrm{G} = 0.01$, $n = 1$, and $\Theta = 50$ K/cm are given in Table 3.

Conclusions. The effect of the thermal expansion of fluids on the occurrence of convection at small Rayleigh numbers, related to the spatial inhomogeneity of the thermal field on the boundaries of the reservoir, is considered for typical substances and the geometrical configurations of physical systems employed in experiments on convection under microgravity and space materials science. The numerical results obtained suggest that in experiments with accelerations 10^5–10^6 times smaller than the acceleration due to terrestrial gravity achievable on modern space vehicles, the contribution of the spatial inhomogeneity of the external thermal field to convection can differ considerably from that obtained for the Boussinesq model.

At the same time, using spatial inhomogeneity of heating, it is possible to effectively study microconvective phenomena in experiments. This approach supplements the approach based on the use of external actions changing rapidly in time. The advantage of the proposed approach is that it makes it possible to form configurations of physical systems such that they favor occurrence of stable, easily predicted qualitative changes in convection regimes generated by the thermal expansion of the medium.

This work was supported by the Siberian Division of the Russian Academy of Sciences (Expertise competition of 2000 of scientific projects of young scientists, Integration Project No. 5) and the Krasnoyarsk Regional Foundation of Science (Grant Nos. 11G26, 12G57, and 13G036).

REFERENCES

1. B. K. Larkin, "Heat flow to a confined fluid in zero gravity," *Progr. Astronaut. Aeronaut.*, **20**, 819–832 (1967).
2. P. G. Grodzka and T. C. Bannister, "Heat flow and convection demonstration experiments aboard Apollo 14," *Science*, **176**, 506–508 (1972).
3. V. V. Pukhnachev, "Model of convective motion under low gravity," *Model. Mekh.*, **6**, No. 4, 47–56 (1992).
4. V. V. Pukhnachev, "Microconvection in a vertical layer," *Izv. Ross. Akad. Nauk, Mekh. Zhidk. Gaza*, No. 5, 76–84 (1994).
5. Yu. V. Lapin and M. Kh. Strelets, *Internal Flows of Gas Mixtures* [in Russian], Nauka, Moscow (1989).
6. D. R. Chenoweth and S. Paolucci, "Natural convection in an enclosed vertical air layer with large horizontal temperature differences," *J. Fluid Mech.*, **169**, 173–210 (1986).
7. P. S. Perera and R. F. Sekerka, "Nonsolenoidal flow in a liquid diffusion couple," *Phys. Fluids*, **9**, No. 2, 376–391 (1997).

8. V. V. Pukhnachov, "Solvability of initial boundary value problem in non-standard model of convection," *Zap. Nauch. Semin. Leningr. Otd. Mat. Inst. Steklova*, **233**, 217–226 (1996).
9. O. N. Goncharova, "Microconvection in weak force fields: A numerical comparison of two models," *J. Appl. Mech. Tech. Phys.*, **38**, No. 2, 219–223 (1997).
10. O. N. Goncharova, "Calculation of microconvection in a long rectangle," *Vychisl. Tekhnol.*, **5**, No. 5, 26–37 (2000).
11. O. N. Goncharova, "Numerical simulation of microconvection in domains with free boundaries," *J. Appl. Mech. Tech. Phys.*, **38**, No. 3, 386–390 (1997).
12. O. N. Goncharova, "Microconvection in domains with free boundaries," *Vychisl. Tekhnol.*, **5**, No. 2, 14–25 (2000).
13. A. A. Amsden and W. F. Harlow, "A simplified MAC technique for incompressible fluid flow calculation," *J. Comput. Phys.*, **6**, No. 2, 322–325 (1970).
14. A. B. Ezerskii, "Dynamics of defects in hexagonal lattices occurring due to Marangoni–Benar convection," in: *Synergetics* (Laboratory Works on Nonlinear Physics) [in Russian], Izd. Udm. Univ., Izhevsk (1999), p. 51–74.